Effect of the Introduction of Polydimethylsiloxane on the Foaming Behavior of Block-Copolymerized Polypropylene

Mingyi Wang,[1] Jun Ma,[1] Raymond Chu,[2] Chul B. Park,[2,3] Zhou Nanqiao[3]

[1]*Mechanical and Electrical Engineering Institute, Zhengzhou University of Light Industry, Zhengzhou 450002, China*
[2]*Microcellular Plastics Manufacturing Laboratory, Department of Mechanical and Industrial Engineering, University of Toronto, Toronto, Ontario M5S 3G8, Canada*
[3]*Key Laboratory of Polymer Processing Engineering, Ministry of Education, National Engineering Research Center of Novel Equipment for Polymer Processing, South China University of Technology, Guangzhou 510640, China*

Received 13 March 2011; accepted 6 May 2011
DOI 10.1002/app.34854
Published online 31 August 2011 in Wiley Online Library (wileyonlinelibrary.com).

ABSTRACT: We investigated the effect of polydimethylsiloxane (PDMS) on the foaming properties of block-copolymerized polypropylene (B-PP) by blending different contents of PDMS with B-PP in the extrusion process using supercritical CO_2 as the blowing agent. The experimental results indicate that the addition of PDMS greatly increased the expansion ratio of the foamed samples. At the same time, the cell population density of foams obtained from the blends also increased to a certain degree and provided a new perspective on improving B-PP's foaming performance. The addition of PDMS also decreased the die pressure because of the reduced viscosity of the B-PP/PDMS blends compared with that of the B-PP matrix. © 2011 Wiley Periodicals, Inc. J Appl Polym Sci 123: 2726–2732, 2012

Key words: block copolymers; blowing agents; compatibility; poly(propylene) (PP); processing

INTRODUCTION

Polypropylene (PP), for which raw material is abundant, is cheap and easily processed. As such, it has become the fastest developing general resin. It has excellent mechanical properties and outstanding stress-cracking resistance, rigidity, heat resistance, and chemical stability. PP resin's chemical structure also makes it recyclable and environmentally friendly. It provides good heat and chemical stability and high mechanical strength. Consequently, PP foam products are widely used in cosmetics and in the packaging of food and electronics. Therefore, PP foam serves as an alternative to polystyrene foam[1–3] in the packaging industry.

Compared with polystyrene and polyethylene, the foaming process for PP is difficult to control. This is mainly because PP is a linear polymer and, as such, possesses a narrow processing window for foaming. Burt[4] reported that the temperature suitable for foaming of PP was only 4°C.

In classical nucleation theory, the nucleation rate is measured in terms of the function of the gas concentration and the interfacial tension between the gas molecules and polymer melts. Either a larger concentration of gas molecules or a smaller interfacial tension between the gas and polymer melts greatly improves the nucleation rate. Research has shown that polydimethylsiloxane (PDMS) has a high CO_2 solubility,[5] a low surface tension, and a high CO_2 infiltration capacity. Therefore, if PDMS is introduced during the extrusion foaming of PP, it is bound to improve PP's foaming properties. However, because the solubility parameter of PDMS is very low, it is difficult for it to be compatible with other polymers. Therefore, compatibilizer must be added[6–12] or the PDMS reunion will lead to large dispersed particles that would seriously deteriorate the performance of the materials. Studies have shown that maleic anhydride grafted polypropylene (PP-*g*-MAH) is an effective compatibilizer for PP/PDMS blends.[6–8] Using a single-screw extruder foaming system and a block copolymer [block-copolymerized polypropylene (B-PP)], we evaluated the influence of PDMS on the PP foaming process by observing the foaming behaviors of several PP/PDMS systems with different concentrations of blended PDMS.

EXPERIMENTAL

Experimental material

The B-PP we used was BA212E, with a melt flow rate (MFR) of 0.3 g/10 min (ISO 1133, 230°C/2.16 kg), from Borealis Gmbh (Austria). PDMS was MB50-001 from Dow Corning Corp. PP-*g*-MAH was

Correspondence to: C. B. Park (park@mie.utoronto.ca).

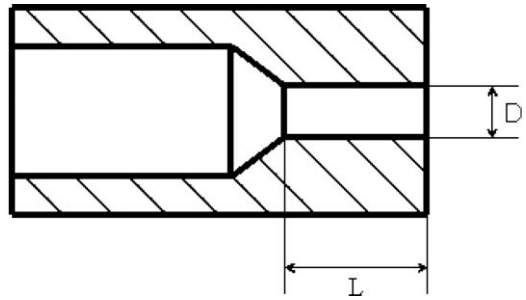

Figure 1 Schematic of the filament die (L = length; D = diameter).

Polygon 3150, with an MFR of 50.0 g/10 min (ASTM D 1238, 230°C/2.16 kg), from Chetrum Corp., and we used supercritical CO_2, with a 99.5% purity, from Linde Co.

Experimental apparatus

Our equipment included a 2697-X hot press from Carver Co. (Orlando, FL), a model D6/2 twin-screw extruder from Brabender Co. (Brabender, Prep Center) with screw diameter of 27 mm, used for the granulation of the blends, and a single-screw extrusion foaming system (Brabender 05-25-000) with a screw diameter of 19.1 mm. For details, see ref. [13]. We also used a differential scanning calorimetry (DSC) instrument (DSC 2910, TA Co.); a Senior ARES rheometer (TA Co.); a sputter coater (model polar SC7620, Quorum Technologies Co., United Kingdom), and a scanning electron microscopy (SEM) instrument (Hitachi 510, Hitachi, Japan).

Sample preparation

First, different concentrations of B-PP, PDMS, and PP-*g*-MAH were put in the high-speed mixing machine for dry mixing, and then, the twin-screw extruder was used to prepare pellets for extrusion foaming. Extrusion foaming experiments were conducted on a single-screw extruder foaming system with a filament die, in which the die channel length was 1 mm and the die diameter was 1.2 mm. The schematic of the filament die used is shown in Figure 1. For extrusion foaming, MFR was kept at 13 g/min. Because of the different feeding rates for the formulations, there were some changes in the screw speed (normally, the screw speed was 25 rpm or greater to ensure a uniform mixture of polymer melts and supercritical CO_2). The supercritical CO_2 amount injected was set at 3% (mass fraction).

Characterization of the foamed samples

Density of the foamed samples

The density of the foamed samples was determined by the buoyancy method. According to the formula $\rho = m/v$, the mass (m) and volume (v) of an object needs to be determined first to measure its density. Because the foamed sample was irregularly shaped, its volume could not be directly measured, and the Archimedes principle was applied.

A beaker filled with distilled water was placed on an electronic scale and contained a metal stent to keep the sample submerged. First, the actual weight of the sample (m) was measured. Then the sample was put under the water, and the readings of the balance (m') were recorded.

The density of the sample was calculated according to the following formula:

$$\rho_f = \frac{m}{m - m'} \rho_{\text{water}} \quad (1)$$

where ρ_f represents the density of the foamed samples and ρ_{water} represents the density of the distilled water.

Cell population density calculation

The foamed samples' cell morphologies were characterized with a scanning electron microscope (model Hitachi 510). All of the foamed samples were dipped into liquid nitrogen and then quickly fractured in air before scanning. The fractured sections were sputter-coated with platinum in a unipolar SC7620 mini sputter coater. The cell size and cell population density were determined by SEM micrographs. We calculated the cell diameter by averaging the sizes of at least 100 cells in the SEM micrographs. For details of the methods used to calculate the cell population density of the foamed samples, see ref. [14].

RESULTS AND DISCUSSION

DSC test results and discussion

All tests were carried out at a heating rate of 10°C/min over a temperature range from 20 to 200°C with nitrogen atmosphere protection. First, the sample temperature was heated from 20 to 200°C, held at 200°C for 5 min to remove the thermal history, then cooled to 20°C with a 10°C/min cooling rate, and finally reheated to 200°C again. DSC thermograms for cooling and the second heating cycle of the B-PP matrix and B-PP/PDMS/PP-*g*-MAH blends are presented in Figure 2. For clarity, the curves have been displaced from the baseline.

Table I shows the DSC test results of the B-PP matrix and B-PP/PDMS/PP-*g*-MAH blends. It further shows that the melting points of the mixtures were higher than those of the B-PP matrix, whereas the crystallization temperatures of the mixtures were lower than those of the B-PP matrix. Therefore, the

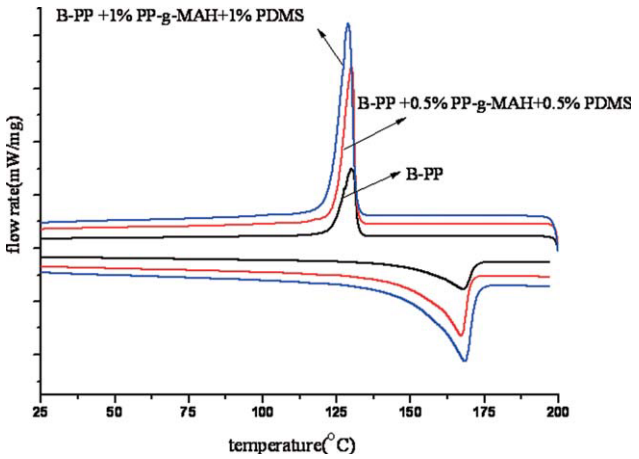

Figure 2 DSC thermograms for cooling and the second heating cycle of the B-PP matrix and the B-PP/PDMS/PP-*g*-MAH blends. [Color figure can be viewed in the online issue, which is available at wileyonlinelibrary.com.]

presence of the compatibilizer PP-*g*-MAH decreased the activity of the PP molecular chain and resulted in a higher melting point. On the other hand, the crystallization temperatures of the PP-*g*-MAH and PDMS were lower than those of the B-PP matrix, which led to a lower crystallization temperature for the blends.

Dynamic shear rheological properties test results and discussion

The dynamic shear rheological properties tests for B-PP and its blends were conducted on a strain-controlled ARES rheometer, with 25-mm parallel-plate geometry and a 1-mm sample gap. Dynamic shear measurements, with frequencies from 0.1 to 70 Hz, were taken at a temperature of 210°C with nitrogen atmosphere protection. Strain was maintained at 10% to ensure linear viscoelasticity.

Figure 3 shows the samples' storage and loss moduli changes within the scanning frequency range. As seen, the addition of PDMS and PP-*g*-MAH decreased the storage and loss moduli of the blends system. With increased PDMS and PP-*g*-MAH in the system, there was a corresponding decrease in the storage and loss moduli. As Figure 4 shows, the complex viscosity of the blends system also lessened with increased PDMS and PP-*g*-MAH. On the one hand, compared with the B-PP matrix, the viscosity of PDMS was low with the role of lubrication. On the other hand, PP-*g*-MAH had a high melt index and low viscosity. Therefore, the viscosity of the blend system decreased with the addition of PDMS and PP-*g*-MAH.

Effect of the die temperature and blend ratio on the foaming expansion ratio of the B-PP/PP-*g*-MAH/PDMS blends

As shown in Figure 5, when the supercritical CO_2 content injected was 3 wt %, the addition of PDMS and PP-*g*-MAH greatly increased the maximum expansion ratio of the foamed samples in the B-PP/PP-*g*-MAH/PDMS blends. This occurred because the addition of PDMS and PP-*g*-MAH provided a large number of nucleation sites and also because the CO_2 solubility in PDMS was much higher than that of PP[5,15,16] and created a huge concentration gradient between the PDMS and PP phases. Consequently, the CO_2 trapped in the PDMS phase could spread to the PP phase through the cell nucleation and growth process; this provided a timely supply of CO_2 for the nucleated bubbles. When the PDMS and PP-*g*-MAH content added was 1 wt % in the blends, the maximum expansion ratio of the foamed samples obtained from the B-PP/PP-*g*-MAH/PDMS blends went up 13 times, whereas the maximum expansion ratio for B-PP foam went up only 7 times. When the PDMS and PP-*g*-MAH content was increased from 0.5 to 1 wt % in the blends, the expansion ratio of the foamed samples increased. In part, this increase occurred because the added PDMS and PP-*g*-MAH provided more nucleating sites, which caused more gas to be used for bubble nucleation and growth. Otherwise, as the viscosity of the B-PP matrix was very high, it prevented cell growth and limited cell expansion. When the PDMS and PP-*g*-MAH content in the blends system increased from 0.5 to 1 wt %, the complex viscosity of the blends decreased; this caused the cells to expand and their walls to thin. The result was a higher expansion ratio for the samples, which indicated that in polymer foaming, a larger viscosity is not necessarily better and that there exists an optimal viscosity value.

TABLE I
Composition of the B-PP/PDMS Blends and the DSC Results

Sample no.	B-PP (wt %)	PP-*g*-MAH	PDMS	T_m (°C)	T_c (°C)
1	100	0	0	167.76	130.13
2	99	0.5	0.5	167.92	129.54
3	98	1	1	168.47	128.97

T_m, melting temperature of the sample; T_c, crystallization temperature.

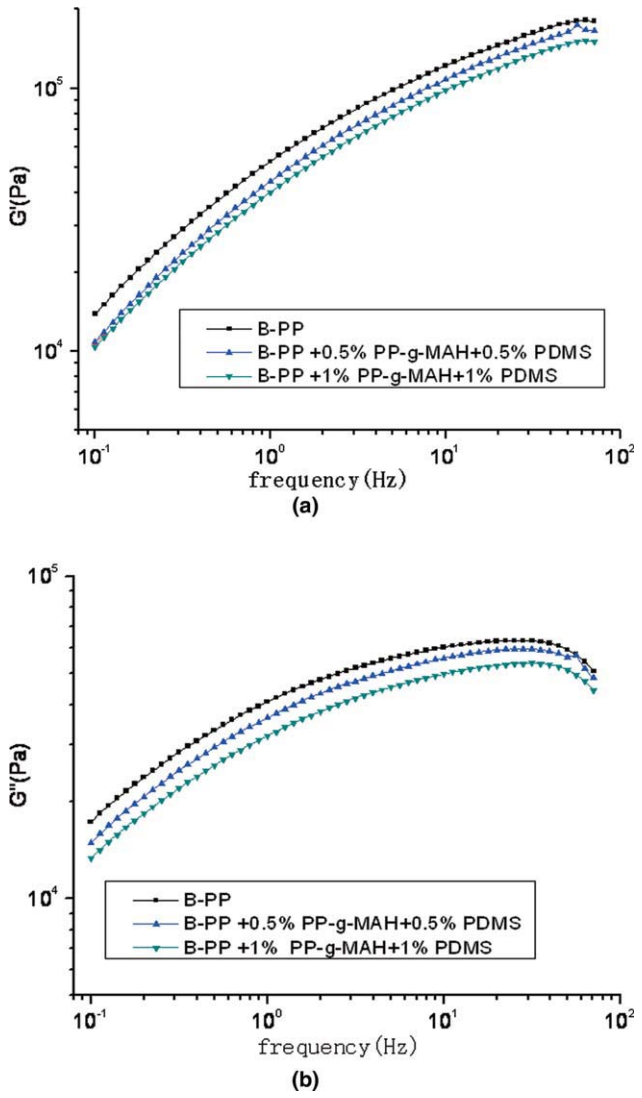

Figure 3 (a) Storage modulus (G') and (b) loss modulus (G'') of B-PP and the B-PP/PP-*g*-MAH/PDMS blend systems. [Color figure can be viewed in the online issue, which is available at wileyonlinelibrary.com.]

Effect of the die temperature and blend ratio on the die pressure in the extrusion foaming process of the B-PP/PP-*g*-MAH/PDMS blends

A lack of die pressure can cause an earlier separation in the gas and polymer melt phase and induce foaming in the die before the polymer melt/gas blends exit the die. Meanwhile, as the internal pressure in small cells is greater than in large cells, the gas tends to diffuse into the earlier formed nucleated cells. This decreases the amount of gas used for cell nucleation and prevents a large number of fine air bubbles from uniformly forming. As a result, large bubbles will appear in the final foamed samples and may even result in hollow foamed samples. Therefore, in the extrusion foaming process, die pressure is extremely important, and it must be higher than the solubility pressure of the foaming agent in the polymer melt under the same conditions. Li et al.[17] studied the solubility of CO_2 in linear/branched PP melts, and we conclude from their findings that the die pressures used in our experiment was higher than the solubility pressures of B-PP.

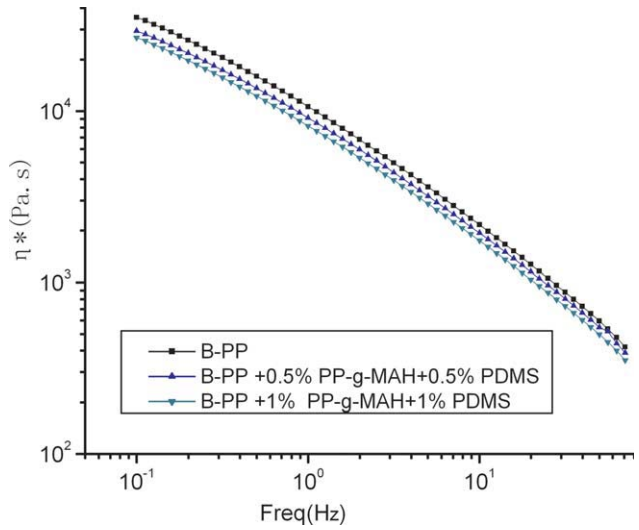

Figure 4 Complex viscosity (η*) of B-PP and the B-PP/PP-*g*-MAH/PDMS blend systems. [Color figure can be viewed in the online issue, which is available at wileyonlinelibrary.com.]

As Figure 6 shows, the introduction of PDMS and PP-*g*-MAH reduced the die pressure, which did not decrease with increased PDMS and PP-*g*-MAH as we had expected. On the contrary, when the PDMS content was increased from 0.5 to 1 wt %, the die pressure increased. The previous DSC results showed that with the increase of PDMS and PP-*g*-MAH content in the blends system, the melting

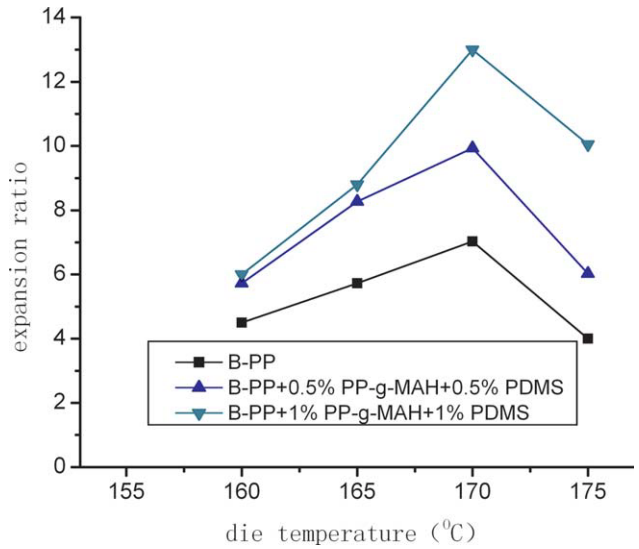

Figure 5 Effect of the die temperature and blend ratio on the expansion ratio of the B-PP/PP-*g*-MAH/PDMS blend foams. [Color figure can be viewed in the online issue, which is available at wileyonlinelibrary.com.]

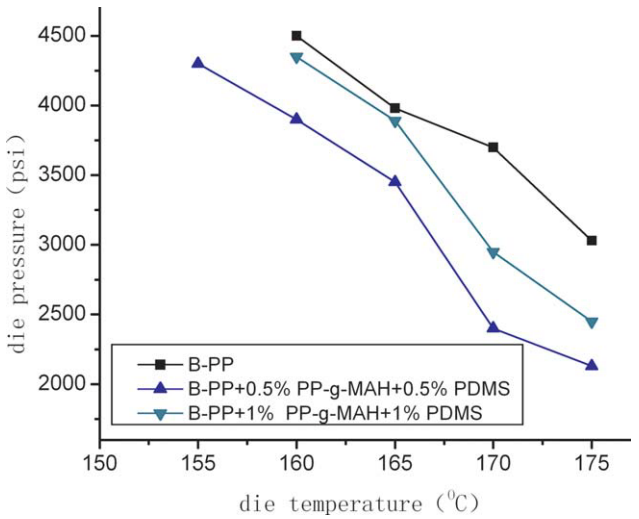

Figure 6 Effect of the die temperature and blend ratio on the die pressure in the extrusion foaming process of the B-PP/PP-*g*-MAH/PDMS blends. [Color figure can be viewed in the online issue, which is available at wileyonlinelibrary.com.]

points of the blends tended to increase. Therefore, the die pressure might have increased because the foaming temperatures of the blends were close to the melting points of the blends so that the increased PDMS and PP-*g*-MAH contents might have caused the increased viscosity in the vicinity of the melting points.

Figure 6 also shows that the lower the die temperature was, the larger the die pressure was in the extrusion foaming process. This was based on the mechanism wherein a lower temperature limits polymer chain activity and results in the blends having a larger viscosity.

Effect of the die temperature and blend ratio on the cell population density of the B-PP/PP-*g*-MAH/PDMS blend foams

Figure 7 shows the effects of the die temperature and blend ratio on the cell population density of the B-PP/PP-*g*-MAH/PDMS foamed samples. Because the CO_2 content injected was 3 wt %, the cell population densities of the foamed samples for the B-PP/PP-*g*-MAH/PDMS blends were higher than those for the pure B-PP foamed samples at all foaming temperatures. The reason for this was that the added PDMS and PP-*g*-MAH provided more nucleation sites that promoted heterogeneous nucleation. Meanwhile, heterogeneous nucleation was also promoted by the poor compatibility of PP and PDMS, for which the free energy barrier was lower at the interface. As the foaming temperature was high, the cell population density of the foamed samples from the B-PP/PP-*g*-MAH/PDMS blends with a blend ratio of 98/1/1 was slightly lower than that of the foamed samples from the B-PP/PP-*g*-MAH/PDMS blends with a blend ratio of 99/0.5/0.5. However, with a decreased foaming temperature, the cell population density of the foamed samples from the B-PP/PP-*g*-MAH/PDMS blends with a blend ratio of 98/1/1 became higher than that of the foamed samples obtained from the B-PP/PP-*g*-MAH/PDMS blends with a blend ratio of 99/0.5/0.5. This was because, with a high foaming temperature, the viscosity of the B-PP/PP-*g*-MAH/PDMS blends with a mass ratio of 98/1/1 decreased to below the 99/0.5/0.5 blend ratio of the PP/PP-*g*-MAH/PDMS blends. Therefore, the interfacial tension was smaller; this made the small bubbles grow into large cells because of the pressure difference inside and outside of them. Because of the great internal pressure within the small bubbles, most of the gas diffused into larger bubbles; this resulted in the disappearance of the small bubbles and in lower cell population densities. As the foaming temperature decreased, the viscosity of the blends increased; this resulted in larger interfacial tension and the survival of small bubbles and higher cell population densities. When the CO_2 solubility of the B-PP/PP-*g*-MAH/PDMS blends with a blend ratio of 98/1/1 was higher than that of B-PP/PP-*g*-MAH/PDMS blends with a blend ratio of 99/0.5/0.5, more CO_2 was used for bubble nucleation. This resulted in a higher cell population density in the samples from the B-PP/PP-*g*-MAH/PDMS blends with a blend ratio of 98/1/1 than in the foamed samples from the 99/0.5/0.5 blend ratio B-PP/PP-*g*-MAH/PDMS blends.

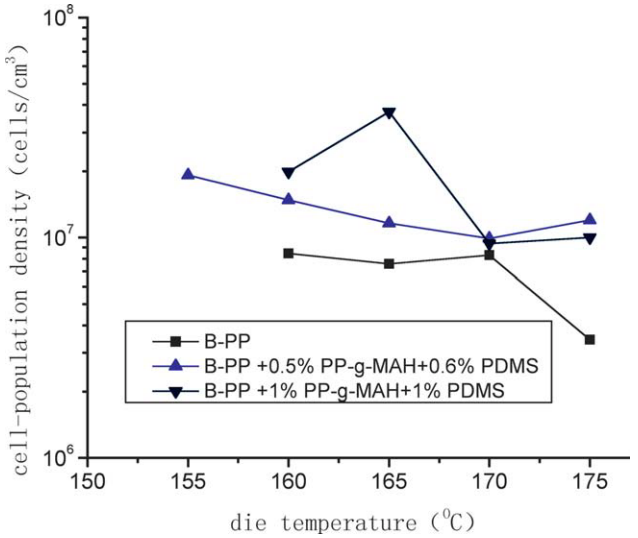

Figure 7 Effect of the die temperature and blend ratio on the cell population density of the B-PP/PP-*g*-MAH/PDMS blend foams. [Color figure can be viewed in the online issue, which is available at wileyonlinelibrary.com.]

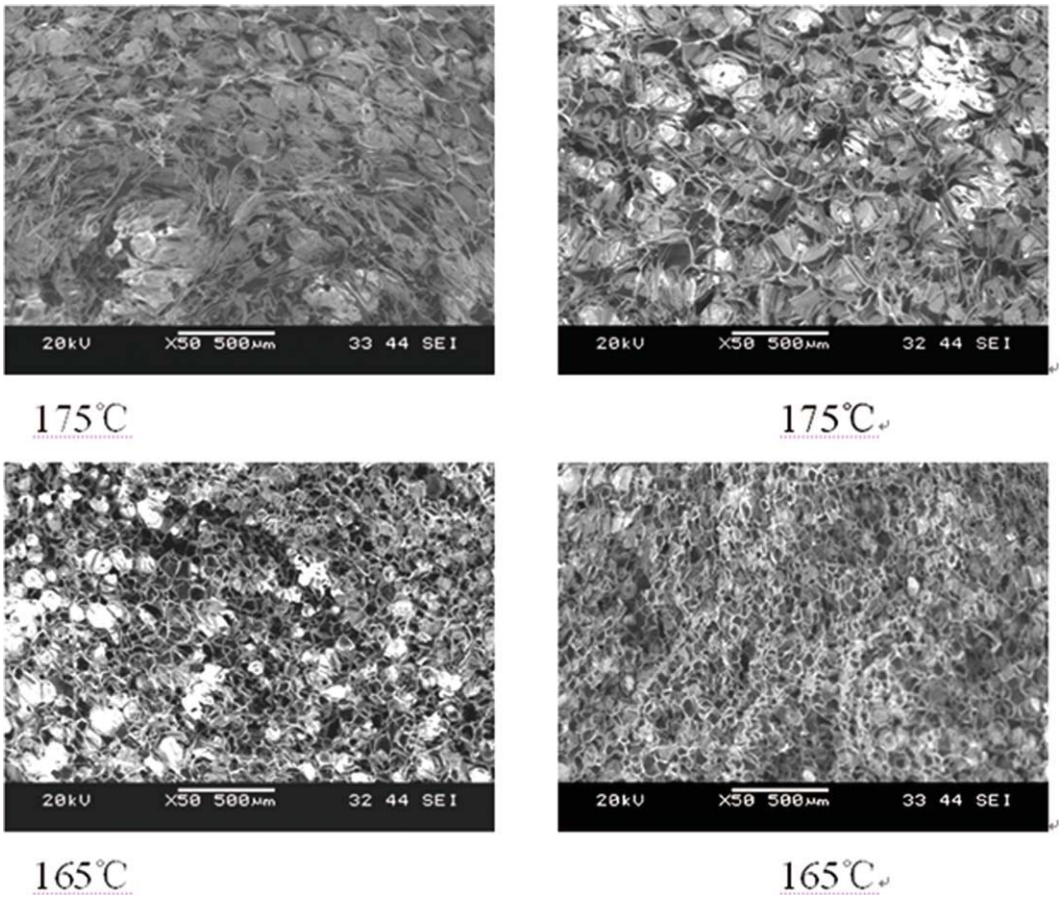

Figure 8 Micrographs of the B-PP matrix foams (left column) and foamed samples from the B-PP/PP-*g*-MAH/PDMS blends (right column) with a blend ratio of 98/1/1 and a CO_2 content of 3 wt %. [Color figure can be viewed in the online issue, which is available at wileyonlinelibrary.com.]

Figure 8 shows cross-sectional micrographs of foamed samples obtained from the B-PP matrix and the B-PP/PP-*g*-MAH/PDMS blends with a weight ratio of 98/1/1. The CO_2 content injected was 3 wt % at different foaming temperatures; this indicated that the addition of PDMS and PP-*g*-MAH increased the cell population density of the foamed samples, especially at lower temperatures.

CONCLUSIONS

1. The curve of the final expansion ratio of the B-PP foam versus the temperature showed a typical mountain shape. This indicated that gas loss at a high temperature and the stiffening of the polymer melt at a low temperature were the two mechanisms that governed the expansion ratio. Therefore, there was an optimum foaming temperature for the semicrystalline polymer.
2. As the CO_2 content injected was 3 wt %, the addition of a small amount of PDMS greatly increased the foam expansion ratio of the samples. The maximum expansion ratio of the foam samples obtained from the PP matrix was just seven-fold, whereas the maximum expansion ratio of foams from the PP/PP-*g*-MAH/PDMS blends with a weight ratio of 98/1/1 was almost 14-fold.
3. The introduction of PDMS and PP-*g*-MAH reduced the die pressure in the extrusion foaming process, but the die pressure did not decrease with increased PDMS and PP-*g*-MAH as we had expected. On the contrary, as the PDMS content increased from 0.5 to 1 wt %, the die pressure increased. Previous DSC results showed that increased PDMS and PP-*g*-MAH content in the blends also tended to increase their melting points. Thus, the increased die pressure might be explained by the blends' foaming temperatures being in the vicinity of the blends' melting points; this means that the increased PDMS and PP-*g*-MAH contents in these might have caused the increased viscosity.

The authors are grateful to Borealis Co. and Dow Corning Co. for providing the B-PP and PDMS, respectively. The authors are also grateful to Zhengzhou University of Light Industry for its financial support (2010BSJJ004).

References

1. Wang, M. C.; Costas, T.; Garry, L. R. J Appl Polym Sci 1996, 61, 1395.
2. Zhang, Q. L.; Sheng, M. Plastics 2002, 31, 41.
3. Lau, H. C.; Bhatacharya, S. N.; Field G. J. Polym Eng Sci 1998, 38, 1915.
4. Burt, J. G. J Cell Plast 1978, 14, 341.
5. Hu, G.; Hoppe, S.; Huang, Y. PPS 2007.
6. Patricia, M.; Werlang, M. J Appl Polym Sci 2007, 104, 226.
7. Prakashan, K.; Gupta, A. K.; Maiti, S. N. J Appl Polym Sci 2007, 105, 2858.
8. Zhai, L.; Zhou, N. Q.; Bu, Y. L.; Wu, Q. F. China Plast Ind 2009, 37, 32.
9. Maric, M.; Macosko, C. W. J Polym Sci Part B: Polym Phys 2002, 40, 346.
10. Li, J. L. Ph.D. Thesis, Shan Dong University, 2006.
11. Patricia, M.; Werlang, M. J Appl Polym Sci 2002, 83, 2347.
12. Park, C. B.; Cheung, L. K.; Patrick, C. L. Cell Polym 1998, 17, 221.
13. Naguib, H. E.; Park, C. B.; Patrick, C. L.; Xu, D. L. J Polym Eng 2006, 26, 565.
14. Baldwin, D. F.; Park, C. B.; Suh, N. P. Polym Eng Sci 1996, 36, 1437.
15. Spitael, P.; Macrosko, C. W.; Mcclurg, R. B. Macromolecules 2004, 37, 6874.
16. Ashok, G.; Esin, G.; Charles, W. M. Macromolecules 1994, 27, 5643.
17. Li, G.; Wang, J.; Park, C. B.; Simha, R. J Polym Sci Part B: Polym Phys 2007, 45, 2497.